

Electronic Supplementary Information (ESI) for

Enhancement of magnetic relaxation properties with 3d diamagnetic cations in [Zn^{II}Ln^{III}] and [Ni^{II}Ln^{III}], Ln^{III} = Kramers lanthanides.

Júlia Mayans,^a Queral Saez,^a Mercè Font-Bardia,^b Albert Escuer,^{*,a}

^a Departament de Química Inorgànica i Orgànica, Secció Inorgànica and Institut de Nanociència i Nanotecnologia (IN²UB), Universitat de Barcelona, Martí i Franqués 1-11, Barcelona-08028, Spain.

^b Departament de Mineralogia, Cristal·lografia i Dipòsits Minerals, Universitat de Barcelona, Martí Franqués s/n, 08028 Barcelona (Spain) and Unitat de Difracció de RX. Centre Científic i Tecnològic de la Universitat de Barcelona (CCiTUB), Solé i Sabarís 1-3. 08028 Barcelona.

Table S1. Crystallographic collection data for complexes **1RR** and **1SS**.

Parameter	1RR	1SS
Formula	$C_{30}H_{26}EuN_5NiO_{13}$	$C_{30}H_{26}EuN_5NiO_{13}$
FW / g mol ⁻¹	875.23	875.23
Crystal system	Monoclinic	Monoclinic
Space group	<i>C2</i>	<i>C2</i>
<i>a</i> / Å	19.125(1)	19.098(1)
<i>b</i> / Å	15.5700(8)	15.5383(7)
<i>c</i> / Å	22.084(1)	22.039(1)
α / °	90	90
β / °	99.096(2)	99.059(2)
γ / °	90	90
<i>V</i> / Å ³	6493.4(6)	6458.5(6)
<i>Z</i>	8	8
<i>T</i> / K	100.0(2)	100.0(2)
ρ_{calc} / g cm ⁻³	1.791	1.800
μ / mm ⁻¹	2.569	2.583
θ range / °	2.016 - 30.603	2.160 - 26.448
Index ranges	$-27 \leq h \leq 27$ $-22 \leq k \leq 22$ $-31 \leq l \leq 31$	$-23 \leq h \leq 23$ $-19 \leq k \leq 18$ $-27 \leq l \leq 27$
Collected reflections	98906	40759
Independent reflections	19717 ($R_{\text{int}} = 0.0700$)	13171 ($R_{\text{int}} = 0.0422$)
Flack parameter	0.13(2)	0.01(2)
Final $R^{b,c}$ indices [$I > 2\sigma(I)$]	$R1 = 0.0387$ $wR2 = 0.0991$	$R1 = 0.0313$ $wR2 = 0.0714$
$(\Delta\rho)_{\text{max,min}}$ / e Å ⁻³	1.956, -1.203	1.038, -0.959

Table S2. Crystallographic collection data for **2RR**, **2SS**, **2SS-b** and **2SS-c**.

Parameter	2RR	2SS	2SS-b	2SS-c
Formula	C ₃₂ H ₃₄ EuN ₅ O ₁₅ Zn	C ₃₂ H ₃₄ EuN ₅ O ₁₅ Zn	C ₆₃ H ₆₄ Eu ₂ N ₁₀ O ₂₉ Zn ₂	C ₃₀ H ₃₀ EuN ₅ O ₁₅ Zn
FW / g mol ⁻¹	945.97	945.97	1859.90	917.92
Crystal system	Monoclinic	Monoclinic	Monoclinic	Monoclinic
Space group	<i>P21</i>	<i>P21</i>	<i>P21</i>	<i>P21</i>
<i>a</i> / Å	9.2811(4)	9.2850(6)	9.209(1)	9.062(1)
<i>b</i> / Å	16.2336(8)	16.239(1)	16.418(3)	17.159(2)
<i>c</i> / Å	23.407(1)	23.453(2)	23.140(4)	22.414(2)
α / °	90	90	90	90
β / °	95.232(2)	95.284(2)	95.496(6)	97.001(4)
γ / °	90	90	90	90
<i>V</i> / Å ³	3512.0(3)	3521.2(4)	3482	3459.1(6)
<i>Z</i>	4	4	2	4
<i>T</i> / K	100.0(2)	100.0(2)	100(2)	100.0(2)
ρ_{calc} / g cm ⁻³	1.789	1.784	1.774	1.763
μ / mm ⁻¹	2.532	2.526	2.551	2.568
θ range / °	2.151 - 30.592	2.148 - 30.558	2.160-25.943	2.544-30.539
Index ranges	-13 ≤ <i>h</i> ≤ 12 -23 ≤ <i>k</i> ≤ 23 -33 ≤ <i>l</i> ≤ 33	-11 ≤ <i>h</i> ≤ 13 -23 ≤ <i>k</i> ≤ 23 -33 ≤ <i>l</i> ≤ 33	-10 ≤ <i>h</i> ≤ 11 -20 ≤ <i>k</i> ≤ 20 -28 ≤ <i>l</i> ≤ 27	-12 ≤ <i>h</i> ≤ 10 -24 ≤ <i>k</i> ≤ 23 -31 ≤ <i>l</i> ≤ 31
Coll. Reflections	149772	117630	31197	42189
Indep. Reflections	21530 ($R_{\text{int}} = 0.0682$)	21475 ($R_{\text{int}} = 0.0308$)	12529 ($R_{\text{int}} = 0.0956$)	18446 ($R_{\text{int}} = 0.0592$)
Flack parameter	0.015(5)	0.017(9)	0.29(4)	0.14(2)
Final <i>R</i> ^{b,c} indices	<i>R</i> 1 = 0.0359	<i>R</i> 1 = 0.0281	<i>R</i> 1 = 0.0737	<i>R</i> 1 = 0.0435
[<i>I</i> >2σ(<i>I</i>)]	w <i>R</i> 2 = 0.0667	w <i>R</i> 2 = 0.0662	w <i>R</i> 2 = 0.1773	w <i>R</i> 2 = 0.0996
(Δρ) _{max,min} / e Å ⁻³	0.991, -1.374	0.968, -2.201	3.731, -2.214	2.672, -2.547

Table S3. SHAPE CShM parameters for the A-molecule of complexes **1RR** and **2SS-c**. The topology for both complexes is intermediate to JSPC-10, SDD-10 and TD-10

			1RR	2SSc
DP-10	D10h	Decagon	36.370	36.223
EPY-10	C9v	Enneagonal pyramid	23.701	25.930
OBPY-10	D8h	Octagonal bipyramid	16.198	15.675
PPR-10	D5h	Pentagonal prism	8.931	11.193
PAPR-10	D5d	Pentagonal antiprism	9.812	12.382
JBCCU-10	D4h	Bicapped cube J15	9.216	10.237
JBCSAPR-10	D4d	Bicapped square antiprism J17	5.134	4.682
JMBIC-10	C2v	Metabidiminished icosahedron J62	6.146	7.348
JATDI-10	C3v	Augmented tridiminished icosahedron J64	17.626	19.313
JSPC-10	C2v	Sphenocorona J87	3.241	3.360
SDD-10	D2	Staggered Dodecahedron (2:6:2)	4.578	3.438
TD-10	C2v	Tetradecahedron (2:6:2)	4.219	2.782
HD-10	D4h	Hexadecahedron (2:6:2) or (1:4:4:1)	6.119	6.986

Table S4. Selected bond parameters for the A-molecule of **2SS-b**.

Eu(1)-O(1)	2.60(2)	Zn(1)-N(1)	2.10(2)
Eu(1)-O(2)	2.41(1)	Zn(1)-N(2)	2.02(2)
Eu(1)-O(3)	2.34(1)	Zn(1)-O(2)	1.96(1)
Eu(1)-O(4)	2.69(2)	Zn(1)-O(3)	2.08(1)
Eu(1)-O(5)	2.48(2)	Zn(1)-O(14)	2.06(2)
Eu(1)-O(6)	2.41(2)	Zn(1)-O(2)-Eu(1)	106.9(6)
Eu(1)-O(8)	2.57(2)	Zn(1)-O(3)-Eu(1)	105.7(6)
Eu(1)-O(9)	2.41(1)	Zn(1)···Eu(1)	3.519(3)
Eu(1)-O(11)	2.52(2)		
Eu(1)-O(12)	2.49(2)		

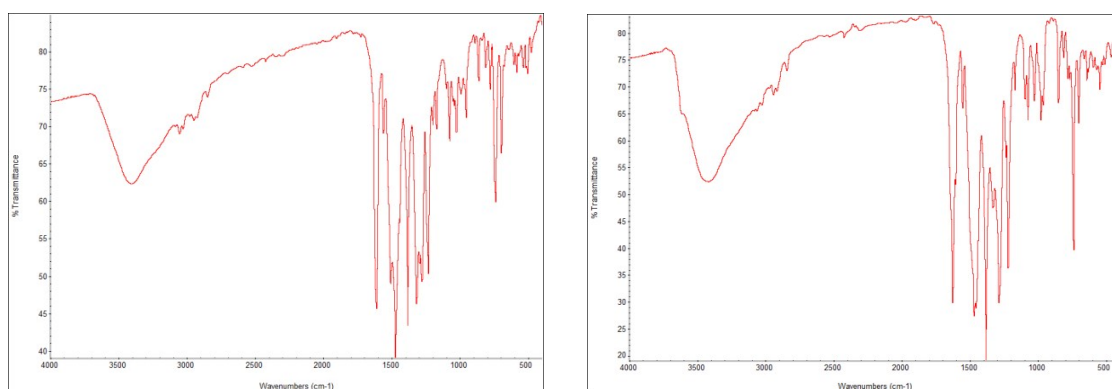


Fig. S1 IR spectra for the representative $[\text{Ni}^{\text{II}}\text{Eu}^{\text{III}}]$ complexes **1** (left) and $[\text{Zn}^{\text{II}}\text{Eu}^{\text{III}}]$ **2** (right). The spectra are similar but not identical due to the different conformation of the phenyl rings of the ligands.

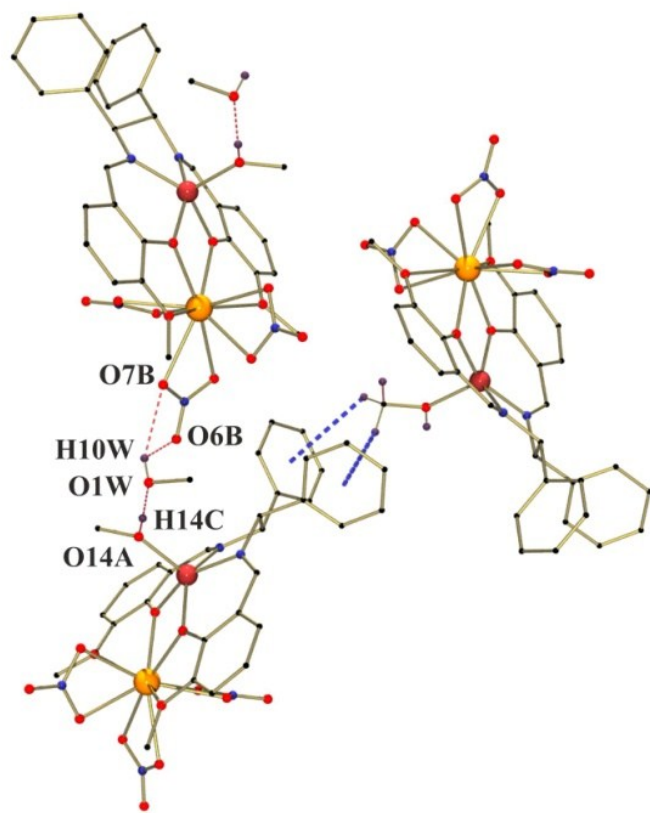


Fig. S2 Intermolecular interactions for complex **2SS**: 1-D arrangement of H-bonds and interchain CH- π (ring) contacts.

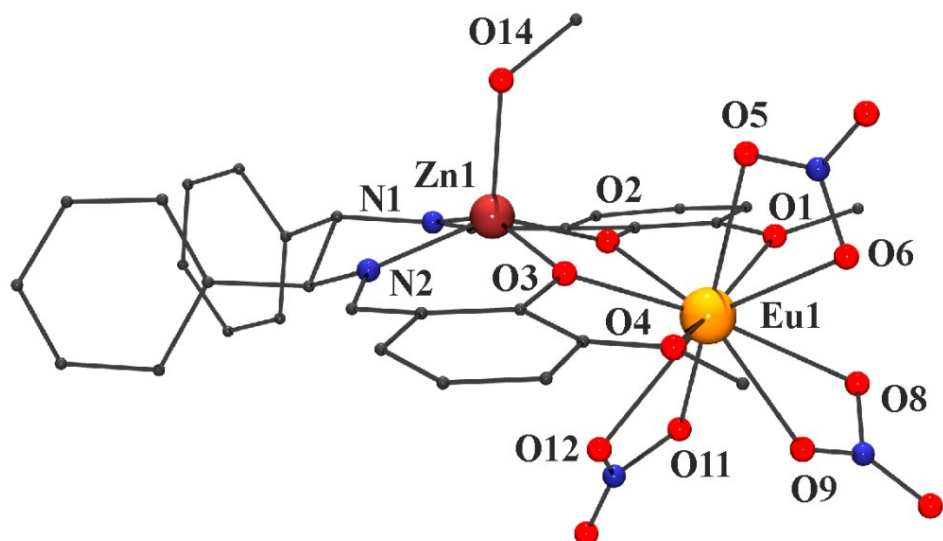


Fig. S3 Labelled view of the A-molecule of structure **2SSb**. At molecular level is practically identical to the structure of the fresh crystal **2SS**. The main differences are found in the intermolecular interactions.

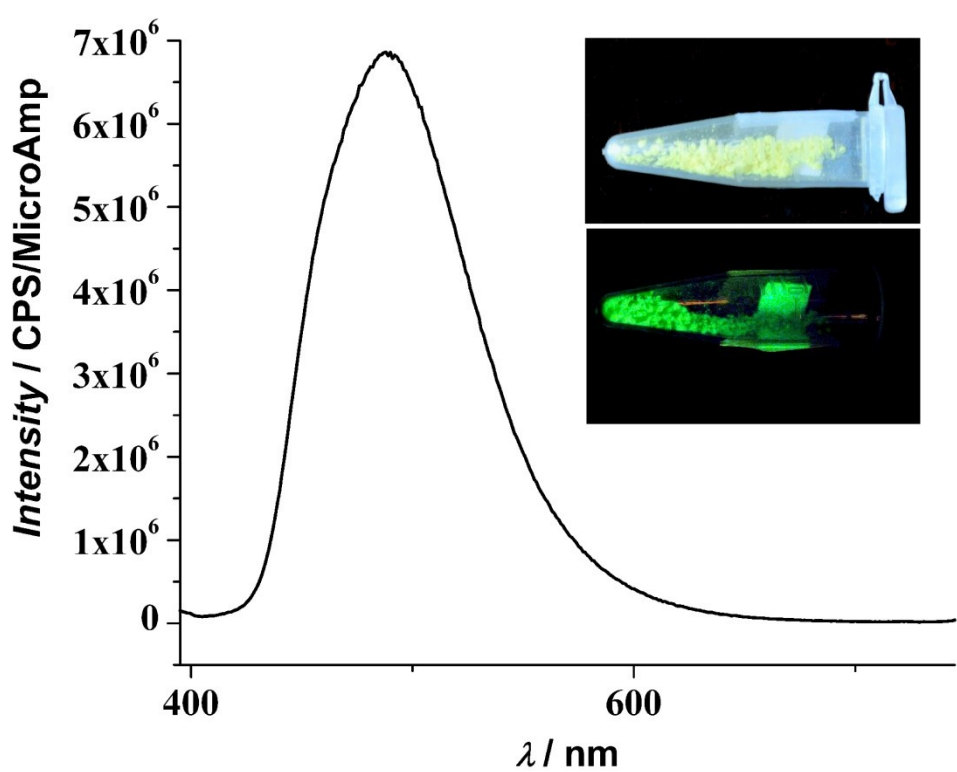


Fig. S4 Emission spectrum for the mononuclear precursor $[\text{Zn}^{II}\text{L}]$. Inset, the sample under white and UV (400 nm) lamp.

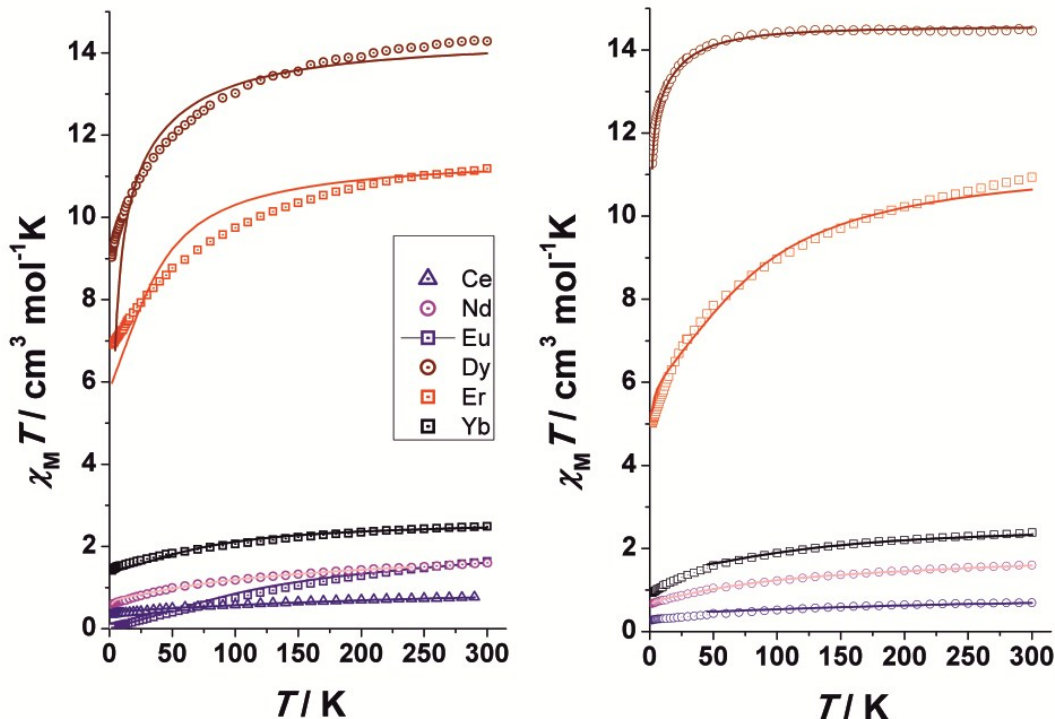


Fig. S5 $\chi_M T$ product vs. Temperature for the $[\text{Ni}^{II}\text{Ln}^{III}]$ (left) and $[\text{Zn}^{II}\text{Ln}^{III}]$ compounds (right). Solid lines show the best simulation.

In our opinion the absolute fit values must be assumed with large caution, but allowed us to give a reliable indication about the sign of Δ , profiting that different Δ sign gives clearly different shaped $\chi_M T$ vs temperature curves, Fig. S5.²⁷

$\Delta > 0$ means that the smallest value of M_J corresponds to the lowest energy state, and so, the lowest spin-orbit $\pm M_J$ states ($\pm 1/2$ for Kramers ions) will be the ground one, while the opposite for $\Delta < 0$. Reasonable fits of the experimental data were reproduced for negative Δ values for Dy^{III} complexes and positive ones for Ce^{III} , Nd^{III} , Er^{III} and Yb^{III} . Although in low symmetry environment, different M_J values can be mixed, and this is probably the reason why the lanthanide Kramers cations with a large number of M_J mixed states have more discrepancies with the fitting Hamiltonian (Dy^{III} and Er^{III}). The method seems to provide a simple alternative to approach the lowest M_J state.

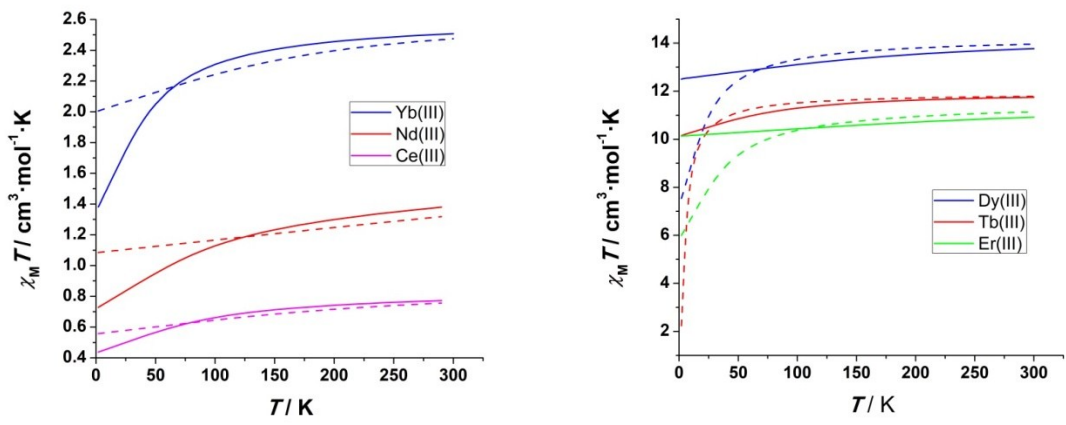


Fig. S6 Simulated $\chi_M T$ plots for a mononuclear Ln^{III} for $\Delta = +25 \text{ cm}^{-1}$ (solid lines) and $\Delta = -25 \text{ cm}^{-1}$ (dotted lines).

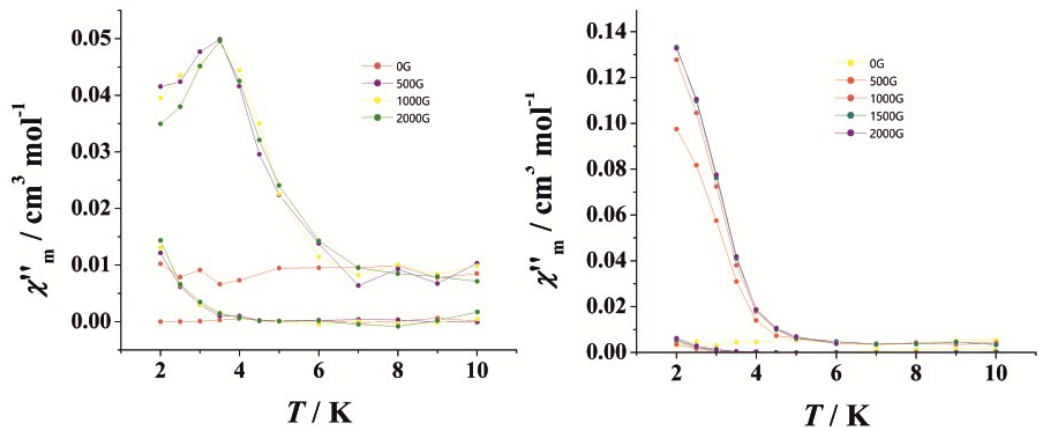
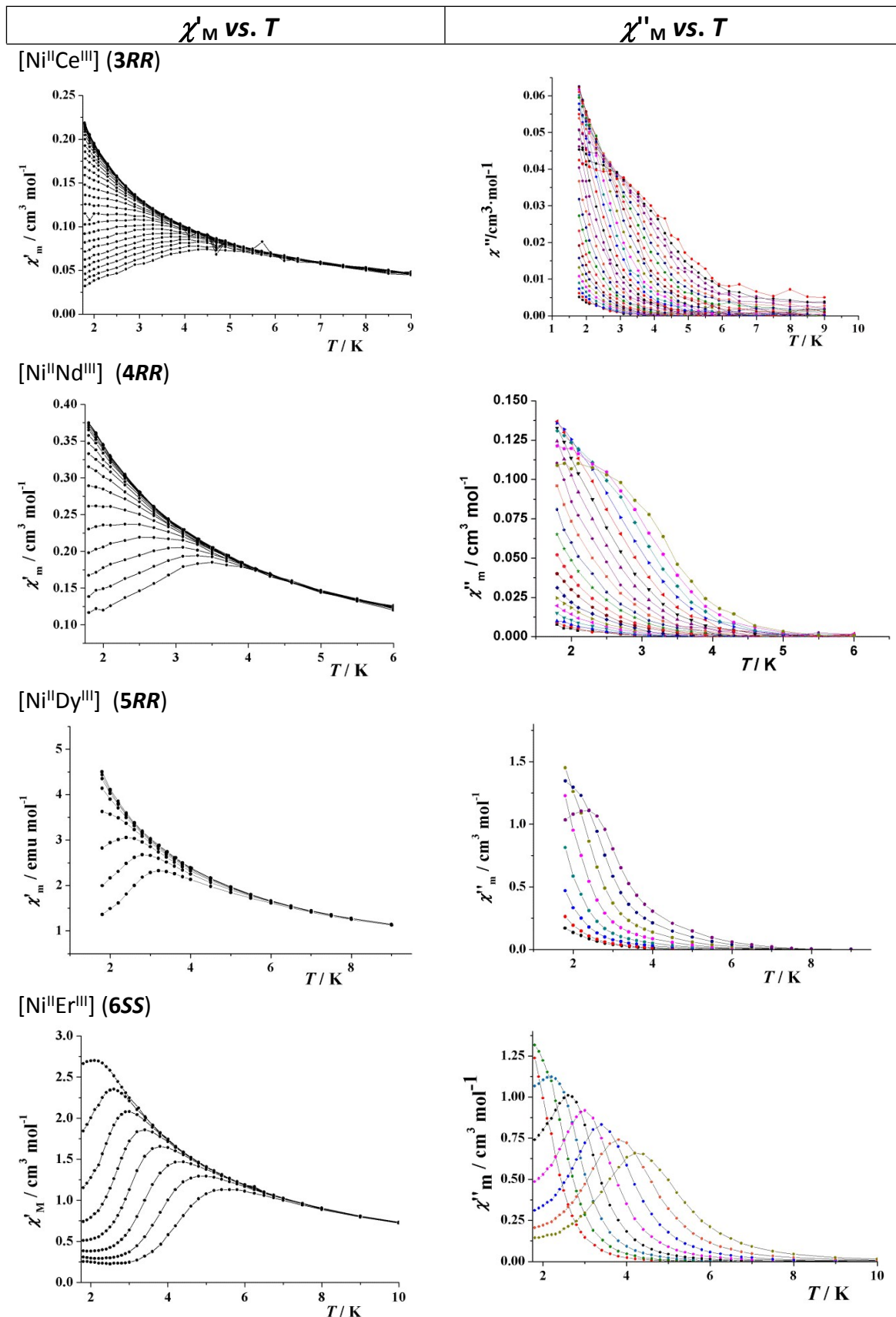


Fig. S7 AC measurements for the $[\text{ZnCe}]$ complex **8** (left) and the $[\text{NiNd}]$ complex **4** (right) at variable field. The field that gives the maximum dependence of the ac signal was selected in all cases to perform the complete measurements.



[Ni^{II}Yb^{III}] (7SS)

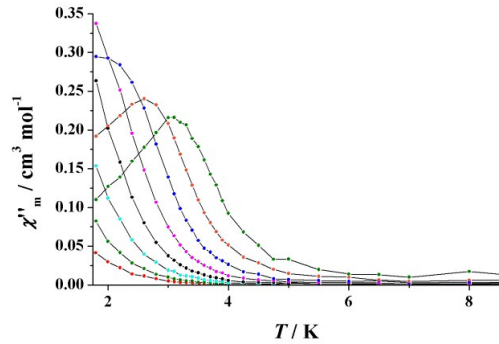
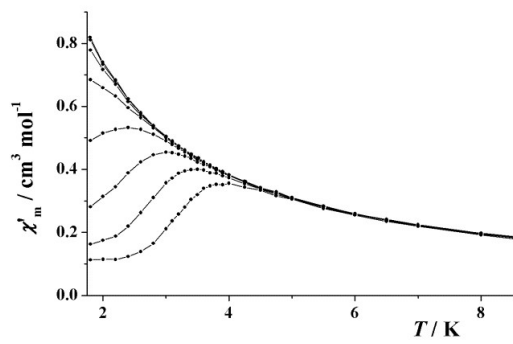


Fig. S8 χ'_M and χ''_M vs. T plots for the [Ni^{II}Ln^{III}] complexes **3 -7**.

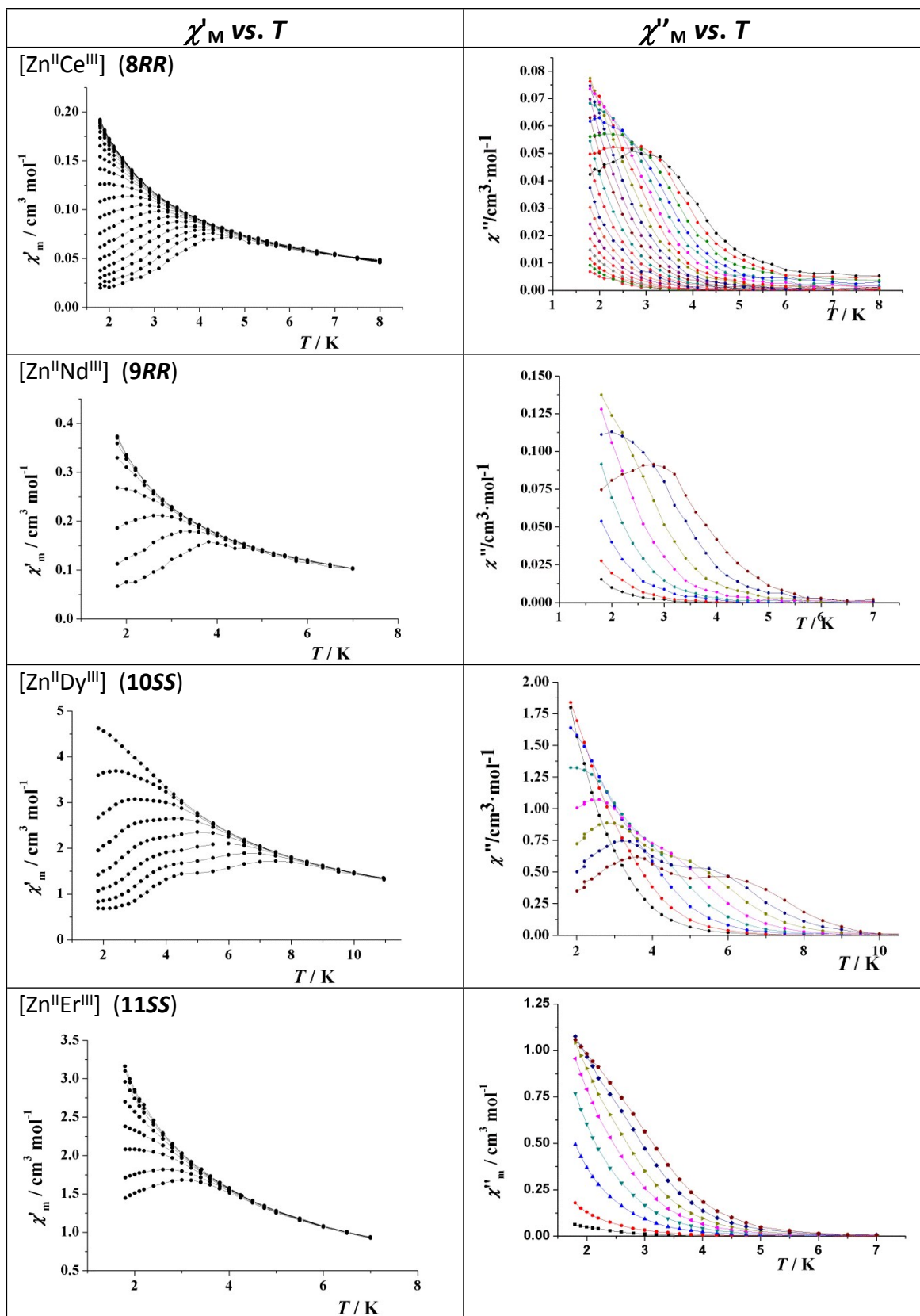


Fig. S9 χ'_M and χ''_M vs. T plots for the $[\text{Zn}^{\text{II}}\text{Ln}^{\text{III}}]$ complexes **8** -**11**. Complex $[\text{Zn}^{\text{II}}\text{Yb}^{\text{III}}]$ (**12**) do not shows ac response.

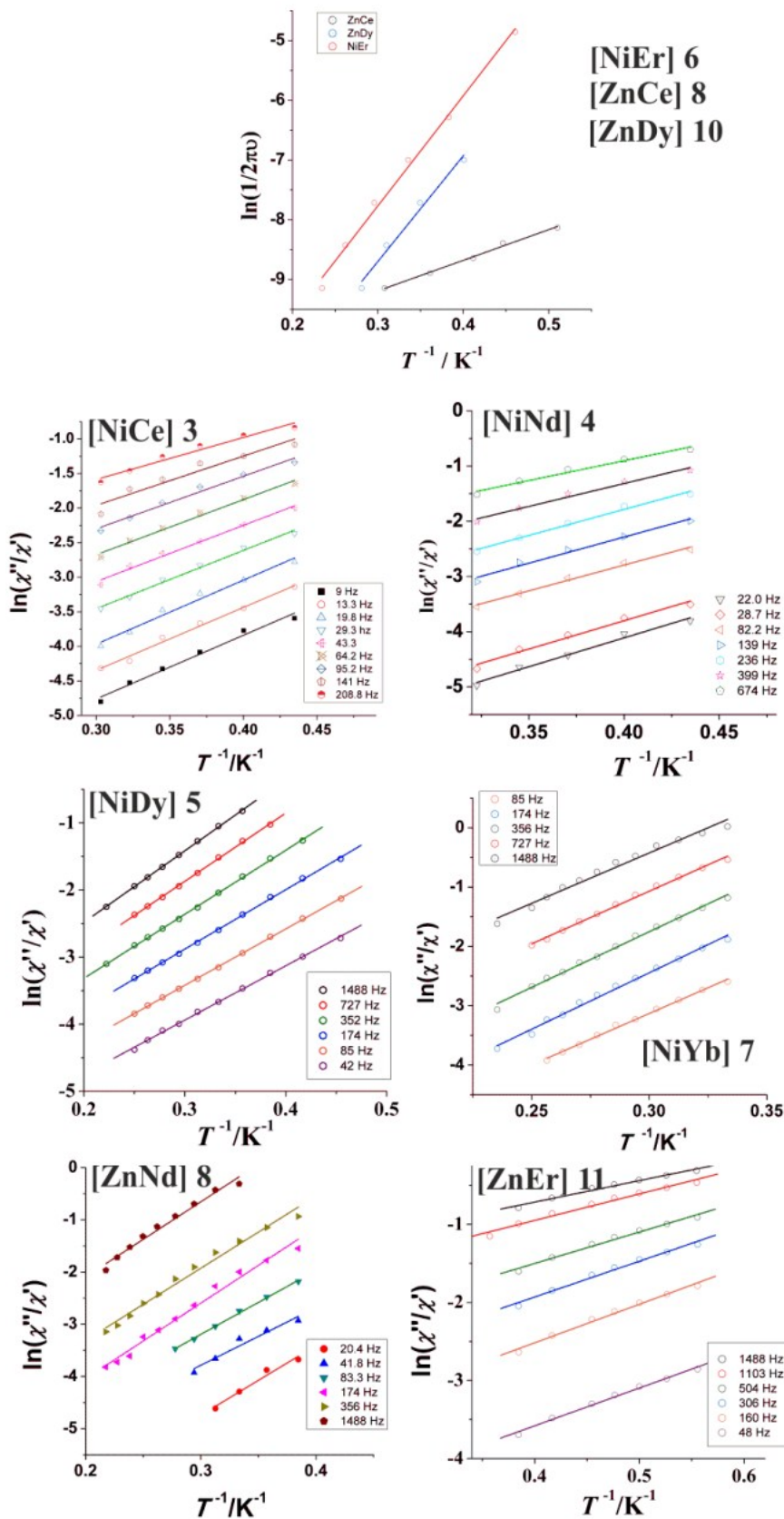


Fig. S10 Fit of the ac data for complexes **6**, **8** and **10** ($\ln(1/(2\pi\omega)) = \ln(1/\tau_0) - U_{\text{eff}}/(k_{\text{B}}T)$) and for **3**, **4**, **5**, **8** and **11** ($\ln(\chi_M''/\chi_M') = \ln(\omega\tau_0) - U_{\text{eff}}/(k_{\text{B}}T)$).

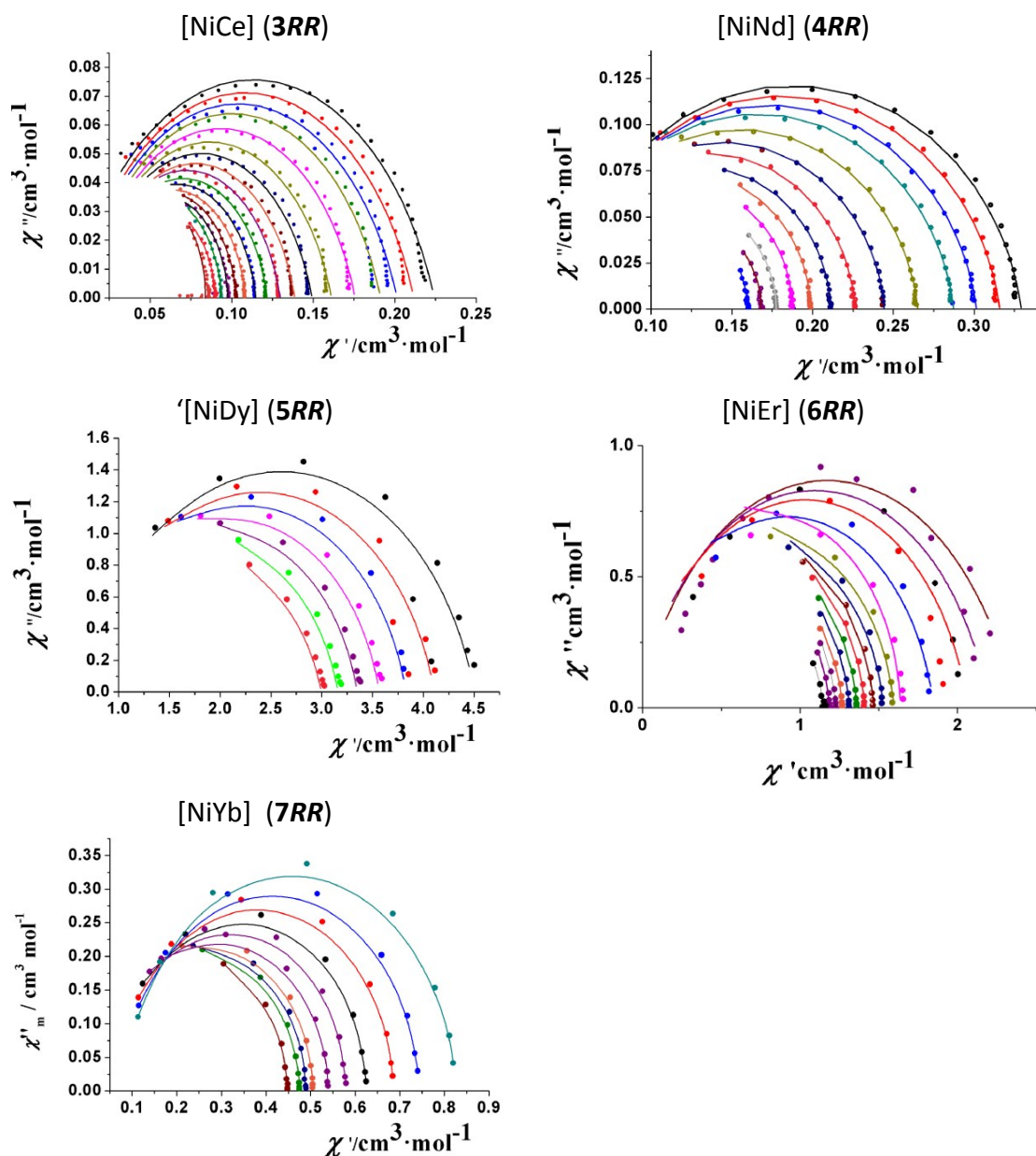


Fig. S11 Cole-Cole plots for the $[\text{Ni}^{\text{II}}\text{Ln}^{\text{III}}]$ complexes **3** -**7** measured in the temperature range 1.8-4.5K. The solid lines represent the best fit.

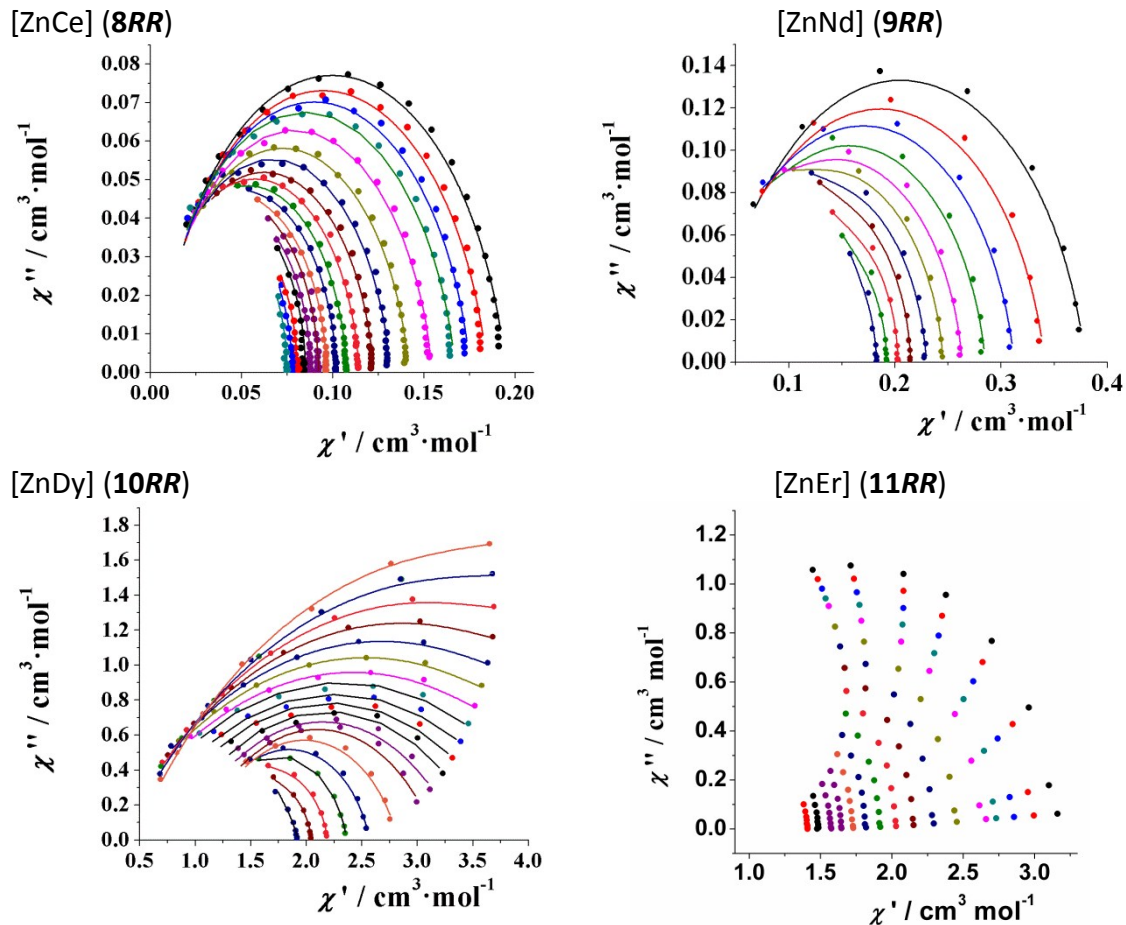


Fig. S12. Cole-Cole plots for the $[\text{Zn}^{II}\text{Ln}^{III}]$ complexes **8** -**11**, measured in the temperature range 1.8-4.5K. The solid lines represent the best fit except for **10** that are eye guide. Data for complex $[\text{Zn}^{II}\text{Er}^{III}]$ (**11**) is not enough to fit the data and complex $[\text{Zn}^{II}\text{Yb}^{III}]$ (**12**) do not shows ac response.

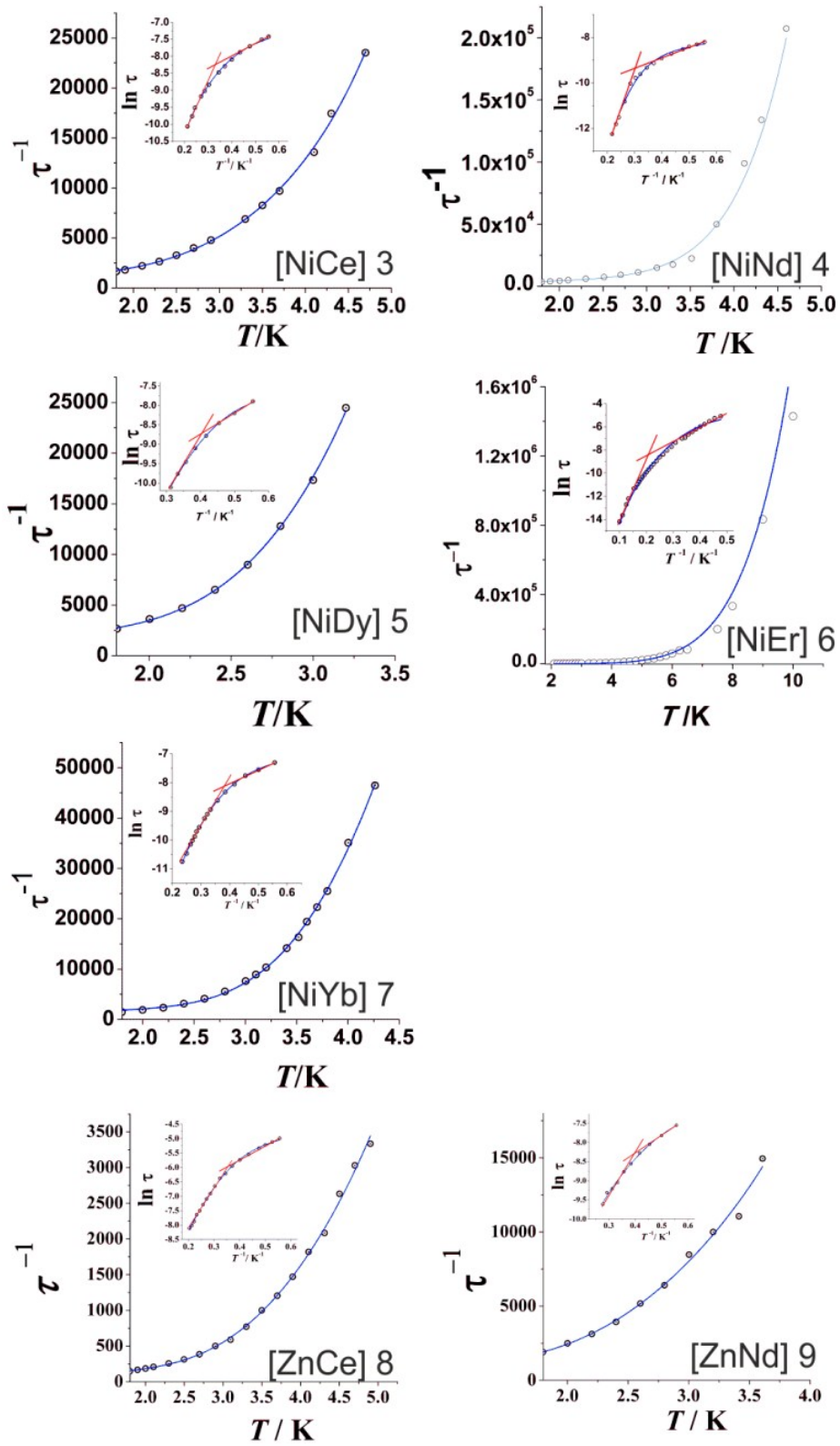


Fig. S13 Dependency of the spin-lattice relaxation temperature obtained from Cole-Cole plots under static dc field as τ^{-1} vs. T or $\ln(\tau)$ vs. T^{-1} (inset). The n values for the term BT^n lies between 6.5-9.1 for all complexes and in agreement with the calculated values by Arrhenius or Debye methods, τ_0 are comprised between 10^{-5} - 10^{-7} .